Journal of
Classical
Analysis
Volume 1, Number 1 (2012), 1–16 doi:10.7153/jca-01-01

THE ASYMPTOTICS OF THE MITTAG–LEFFLER POLYNOMIALS

R. B. PARIS

Abstract. We investigate the asymptotic behaviour of the Mittag-Leffler polynomials $G_n(z)$ for large n and z, where z is a complex variable satisfying $0 \leqslant \arg z \leqslant \frac{1}{2}\pi$. A summary of the asymptotic properties of $G_n(ix)$ for real values of x and an approximation for its extreme zeros as $n \to \infty$ are given. When the variables are such that z/n is finite, an expansion is obtained using the method of steepest descents applied to a suitable integral representation. This expansion holds everywhere in the first quadrant of the z-plane except in the neighbourhood of the point $z = in$, where there is a coalescence of saddle points. Numerical results are presented to illustrate the accuracy of the various expansions.

1. Introduction

The Mittag-Leffler polynomials $G_n(z)$ occur as the coefficients in the expansion

$$\left(\frac{1+t}{1-t}\right)^z = \sum_{n=0}^{\infty} G_n(z)t^n \qquad (|t| < 1), \tag{1.1}$$

and have the representation [1]

$$G_n(z) = 2z\,{}_2F_1\left(\begin{matrix}1-n, 1-z\\ 2\end{matrix}\middle|\, 2\right) \qquad (n \geqslant 1), \tag{1.2}$$

where ${}_2F_1$ denotes the Gauss hypergeometric function; see also [11, §4.1.6], [5]. These polynomials satisfy the recurrence relation

$$(n+1)G_{n+1}(z) = (n-1)G_{n-1}(z) + 2zG_n(z) \qquad (n \geqslant 1)$$

with the starting values $G_{-1}(z) = 0$, $G_0(z) = 1$ and are polynomials in z consisting of even (resp. odd) powers of z according as n is even (resp. odd). The first few polynomials are

$$\begin{aligned}
&G_1(z) = 2z, \quad G_2(z) = 2z^2\\
&G_3(z) = \tfrac{1}{3}z(2+4z^2)\\
&G_4(z) = \tfrac{1}{3}z^2(4+2z^2)\\
&G_5(z) = \tfrac{1}{15}z(6+20z^2+4z^4)\\
&G_6(z) = \tfrac{1}{45}z^2(46+40z^2+4z^4)
\end{aligned}$$

Mathematics subject classification (2010): Primary 41A60, 33C45.
Keywords and phrases: Mittag-Leffler polynomials, asymptotic expansion, uniform approximation, extreme zeros.

Paper JCA-01-01

which are seen to possess the leading term $(2z)^n/n!$. A recent study of these polynomials together with a generalisation can be found in [13]. An application of the Mittag-Leffler polynomials applied to an expansion for the Riemann zeta function is discussed in [12].

When the variable z is purely imaginary (we put $z \mapsto ix$, x real), $G_n(ix)$ possesses an orthogonal polynomial structure. The $G_n(ix)$ are related to the symmetric Meixner–Pollaczek polynomials $P_n^{(\lambda)}(x)$, which are defined by the generating function

$$(1+it)^{-\lambda-ix}(1-it)^{-\lambda+ix} = \sum_{n=0}^{\infty} P_n^{(\lambda)}(x)t^n \qquad (|t|<1).$$

The $P_n^{(\lambda)}(x)$ have the explicit representation

$$P_n^{(\lambda)}(x) = \frac{(2\lambda)_n i^n}{n!}\,{}_2F_1\left(\left.\begin{array}{c}-n, \lambda+ix\\ 2\end{array}\right| 2\right),$$

where $(a)_n = \Gamma(a+n)/\Gamma(a)$ is Pochhammer's symbol, from which it easily follows by (1.2) that

$$G_n(ix) = \frac{2i^n x}{n} P_{n-1}^{(1)}(x). \tag{1.3}$$

An asymptotic expansion for the Meixner–Pollaczek polynomials as $n \to \infty$, which holds uniformly for finite real values of x, has been obtained in [6] in terms of the parabolic cylinder function and its derivative.

In this paper we present a summary of the main asymptotic properties of $G_n(ix)$ for real x as $n \to \infty$, including an approximation for its extreme zeros. We give expansions for $G_n(z)$ when $|z| \to \infty$, n finite and $n \to \infty$, z finite by writing the hypergeometric function in (1.2) in different forms suitable for computation in these two limiting cases. Our main purpose, however, is to consider the asymptotic expansion of $G_n(z)$ in (1.2) for large n and large complex values of z such that $\xi \equiv z/n$ is finite. This is obtained by a routine application of the method of steepest descents applied to a suitable integral representation. Since

$$G_n(-z) = (-)^n G_n(z), \qquad G_n(\overline{z}) = \overline{G_n(z)}, \tag{1.4}$$

where the bar denotes the complex conjugate, it is clearly sufficient to restrict our attention to the first quadrant $0 \leqslant \arg z \leqslant \frac{1}{2}\pi$.

2. Summary of the non-uniform approximations for $G_n(in\xi)$, $\xi > 0$

In this section we collect together various useful asymptotic properties of $G_n(z)$ when $z = ix$, with $x > 0$. These polynomials satisfy the orthogonality property given by [2]

$$\int_{-\infty}^{\infty} G_n(ix)G_m(-ix)\,\frac{dx}{x\sinh \pi x} = \frac{2}{n}\,\delta_{nm}$$

for non-negative integers n and m, where δ_{nm} is the Kronecker delta symbol.

In [6], Li and Wong gave a uniform asymptotic expansion for the more general Meixner-Pollaczek polynomial $M_n(2x;\delta,\eta)$ for real values of the variable x in terms of the parabolic cylinder function and its derivative. The symmetrical Meixner-Pollaczek polynomial $P_n^{(\lambda)}(x)$ that interests us here is given by

$$P_n^{(\lambda)}(x) = \frac{1}{n!} M_n(2x;0,2).$$

In Section 6, Li and Wong gave various non-uniform approximations for $M_n(2x;\delta,\eta)$ obtained from their uniform expansion. If we set $\xi = x/n$, then with $\delta = 0$, $\eta = 2$ and the parameters defined in their paper $r_0 = 1$, $\alpha_+ = 2$, $\theta_0 = \frac{1}{2}\pi$, $\alpha = 2\xi$ and

$$w_\pm = \xi \pm \sqrt{\xi^2 - 1} \qquad (\xi > 1),$$

we obtain from (6.9), (6.23) and (6.37) of [6], and (1.3), the leading behaviour as $n \to \infty$ given by[1]

$$G_n(in\xi) \sim \begin{cases} \dfrac{2i^n}{\sqrt{2\pi n}} \dfrac{\xi^{\frac{1}{2}} e^{\frac{1}{2}\pi n\xi}}{(1-\xi^2)^{\frac{1}{4}}} \sin\left[n\theta - n\xi \log(\xi^{-1} + \sqrt{\xi^{-2}-1}) + \dfrac{1}{4}\pi\right] & (0 < \xi < 1) \\[2ex] \dfrac{2^{1/3} 3^{-2/3} i^n}{n^{1/3}\Gamma(\frac{2}{3})} e^{\frac{1}{2}\pi n} & (\xi = 1) \\[2ex] \dfrac{i^n}{\sqrt{2\pi n}} \dfrac{\xi^{\frac{1}{2}} e^{\frac{1}{2}\pi n\xi}}{(\xi^2-1)^{\frac{1}{4}}} \exp\left[n(\theta - \xi \arctan\sqrt{\xi^2-1})\right] & (\xi > 1), \end{cases} \tag{2.1}$$

where

$$\theta = \arccos\xi \quad (0 < \xi < 1), \qquad \theta = \operatorname{arccosh}\xi \quad (\xi > 1). \tag{2.2}$$

We remark that the first and third expressions in (2.1) may also be obtained from the leading terms of the expansions in (4.11).

From Section 1 it is clear that $G_n(z)$ is a polynomial in z of degree n, with a double (resp. simple) zero at the origin when n is even (resp. odd). From the uniform approximation for the Meixner-Pollaczek polynomial in terms of the Airy function Ai given in [6, (6.23)], it is clear that $G_n(in\xi)$ has zeros in $-1 < \xi < 1$; by symmetry, it is sufficient to consider only $0 < \xi < 1$. There are thus N positive zeros, where $N = \frac{1}{2}n - 1$ or $\frac{1}{2}n - \frac{1}{2}$ according as n is even or odd, respectively.

Let us denote the kth positive zero of $G_n(in\xi)$ by $\xi_{n,k}$, where the zeros are enumerated in decreasing order by $\xi_{n,1} > \xi_{n,2} > \ldots > \xi_{n,N}$. A three-term asymptotic approximation for the zeros as $n \to \infty$ can be obtained from [6, (7.17)] as

$$\xi_{n,k} = 1 + 2^{-1/3} a_k n^{-2/3} + (1 - 2^{-4/3}) n^{-1} + O(n^{-4/3}), \tag{2.3}$$

[1] In the third formula in (2.1), we have written the factor $\exp[2n\xi \arctan(\xi - \sqrt{\xi^2-1})]$ appearing in [6, (6.9)] in the equivalent form $\exp[n\xi(\frac{1}{2}\pi - \arctan\sqrt{\xi^2-1})]$.

where a_k denotes the kth negative zero of Ai(x). From [9, p. 201], we have the approximate values $a_k \simeq -(\frac{3}{2}\pi(k-\frac{1}{4}))^{2/3}$ $(k=1,2,\ldots)$. It is worth pointing out that the leading approximation for the extreme zeros (k finite)

$$\xi_{n,k} \simeq 1-\left(\frac{3\pi}{2\sqrt{2n}}(k-\tfrac{1}{4})\right)^{2/3} \qquad (n\to\infty)$$

follows from a routine calculation using the first non-uniform approximation in (2.1). The gap between the extreme zeros and the endpoint $\xi=1$ is thus seen to be $O(n^{-2/3})$.

In Table 1 we show the values of $\xi_{n,k}$ computed from (2.3), employing the values of the negative zeros a_k given in [9, p. 201], compared with the numerically computed zeros obtained from (1.2) by the Newton-Raphson method.

	$n=50$		$n=80$	
k	$\xi_{n,k}$	Asymptotic	$\xi_{n,k}$	Asymptotic
1	0.866390	0.87533	0.901715	0.90759
2	0.770636	0.77300	0.830400	0.83278
3	0.695015	0.68922	0.773469	0.77154
4	0.630317	0.61517	0.724263	0.71741
5	0.572974	0.54749	0.680211	0.66793

Table 1: *Values of the first five positive zeros ξ_k for different values of n and their asymptotic approximation.*

3. The expansion of $G_n(z)$ for large z or large n

To obtain the expansions of $G_n(z)$ for large z, with n finite, and large n, with z finite, we make use of the transformation for nonnegative integer n

$$ {}_2F_1\left(\begin{matrix}-n,b\\c\end{matrix}\middle| z\right)=(-z)^n\frac{(b)_n}{(c)_n}\,{}_2F_1\left(\begin{matrix}-n,1-n-c\\1-n-b\end{matrix}\middle|\frac{1}{z}\right) \tag{3.1}$$

provided $b\neq 0,-1,\ldots,-n+1$ (unless $b=c$). This result follows by writing the series expansion of the hypergeometric function on the left-hand side of (3.1) in ascending powers of z and reversing the order of summation by replacing the summation index r by $n-r$. Application of (3.1) to (1.2) then yields

$$G_n(z)=\frac{(-2)^n\Gamma(n-z)}{n!\Gamma(-z)}\,{}_2F_1\left(\begin{matrix}1-n,-n\\1+z-n\end{matrix}\middle|\tfrac{1}{2}\right) \tag{3.2}$$

$$=\frac{(-2)^n\Gamma(n-z)}{n!\Gamma(-z)}\sum_{r=0}^{n-1}\binom{n}{r}\binom{n-1}{r}\frac{2^{-r}r!}{(1+z-n)_r} \tag{3.3}$$

for[2] $z\neq 1,2,\ldots,n-1$, which is in the form of a convergent inverse factorial expansion suitable for computation when $|z|\to\infty$. We observe that since

$$\frac{(-2)^n\Gamma(n-z)}{n!\,\Gamma(-z)}=\frac{(2z)^n}{n!}\prod_{r=1}^{n-1}\left(1-\frac{r}{z}\right),$$

the leading behaviour of $G_n(z)$ is verified to be $(2z)^n/n!$ as $|z|\to\infty$.

An alternative representation of $G_n(z)$ can be obtained by applying the well-known linear transformation [9, Eq. (15.8.1)]

$$ {}_2F_1\left(\left.{a,b \atop c}\right| z\right)=(1-z)^{c-a-b}\,{}_2F_1\left(\left.{c-a,c-b \atop c}\right| z\right) \tag{3.4}$$

to (3.2) to yield

$$G_n(z)=(-)^n\frac{2^{-z}\Gamma(n-z)}{n!\,\Gamma(-z)}\,{}_2F_1\left(\left.{z,1+z \atop 1+z-n}\right| \tfrac{1}{2}\right). \tag{3.5}$$

If we now apply the second linear transformation [7, Ch. 3]

$$ {}_2F_1\left(\left.{a,b \atop c}\right| z\right)=A\,{}_2F_1\left(\left.{a,b \atop a+b-c+1}\right| 1-z\right)-\frac{Bz^{1-c}}{(1-z)^{a+b-c}}\,{}_2F_1\left(\left.{1-a,1-b \atop 2-c}\right| z\right), \tag{3.6}$$

where

$$A=\frac{\Gamma(a-c+1)\Gamma(b-c+1)}{\Gamma(a+b-c+1)\Gamma(1-c)},\qquad B=\frac{\Gamma(c-1)\Gamma(a-c+1)\Gamma(b-c+1)}{\Gamma(a)\Gamma(b)\Gamma(1-c)},$$

this enables us to express the hypergeometric function in (3.5), with $-n$ in the denominatorial parameter, in terms of two similar hypergeometric functions, with $+n$ in the denominatorial parameter. Thus, we obtain

$$ {}_2F_1\left(\left.{z,1+z \atop 1+z-n}\right| \tfrac{1}{2}\right)=$$

$$\frac{\Gamma(n)\,\Gamma(n+1)}{\Gamma(n-z)\,\Gamma(1+z)}\left\{\frac{1}{(1+z)_n}\,{}_2F_1\left(\left.{z,1+z \atop 1+z+n}\right| \tfrac{1}{2}\right)+\frac{(-)^{n-1}2^{2z}}{(1-z)_n}\,{}_2F_1\left(\left.{-z,1-z \atop 1-z+n}\right| \tfrac{1}{2}\right)\right\}.$$

This last result yields the representation

$$G_n(z)=\Gamma(n)\Big\{\Upsilon_n(-z)+(-)^n\Upsilon_n(z)\Big\}, \tag{3.7}$$

where we have defined

$$\Upsilon_n(z)\equiv\frac{2^{-z}}{\Gamma(1+z+n)\,\Gamma(-z)}\,{}_2F_1\left(\left.{z,1+z \atop 1+z+n}\right| \tfrac{1}{2}\right).$$

[2]For $z=1,2,\ldots,n-1$ the limiting form of (3.3) would have to be taken.

The expansion of $G_n(z)$ for $n\to\infty$ now follows from (3.7), since the hypergeometric function appearing in $\Upsilon_n(z)$ can be written as a convergent inverse factorial expansion to produce

$$\Upsilon_n(z)=\frac{2^{-z}}{\Gamma(-z)}\sum_{r=0}^\infty \frac{(z)_r(1+z)_r 2^{-r}}{\Gamma(1+z+n+r)\,r!}$$

suitable for computation in the limit $n\to\infty$.

The leading behaviour of $G_n(z)$ as $n\to\infty$ can be obtained from (3.7) by application of the standard result

$$\frac{\Gamma(n+a)}{\Gamma(n+b)}=n^{a-b}(1+O(n^{-1}))\qquad (n\to\infty)$$

to yield

$$G_n(z)=\frac{2^z n^{z-1}}{\Gamma(z)}(1+O(n^{-1})+O(n^{-2z}))\qquad (n\to\infty) \tag{3.8}$$

when Re $(z)>0$. In the particular case $\arg z=\frac{1}{2}\pi$, we replace z by ix (with $x>0$) to find

$$\begin{aligned}G_n(ix)&=\left(\frac{2^{ix}n^{ix-1}}{\Gamma(ix)}+(-)^n\frac{2^{-ix}n^{-ix-1}}{\Gamma(-ix)}\right)(1+O(n^{-1}))\\ &=\frac{2e^{\pi in/2}}{n}\left(\frac{x\sinh\pi x}{\pi}\right)^{1/2}\cos\left[x\log(2n)-\Psi(x)-\frac{1}{2}\pi n\right](1+O(n^{-1}))\end{aligned} \tag{3.9}$$

as $n\to\infty$, where $\Psi(x)=\arg\Gamma(ix)$ and we have made use of the standard result $|\Gamma(ix)|=(\pi/x\sinh\pi x)^{1/2}$.

4. The expansion of $G_n(z)$ for large z and n

From the generating relation in (1.1) it follows by Cauchy's theorem that

$$G_n(z)=\frac{1}{2\pi i}\oint\left(\frac{1+t}{1-t}\right)^z\frac{dt}{t^{n+1}},$$

where the integration path is a small closed curve surrounding the origin in the positive sense. We introduce the variable $\xi\equiv z/n$, where it is sufficient by (1.4) to restrict attention to the first quadrant $0\leqslant\arg\xi\leqslant\frac{1}{2}\pi$. Then

$$G_n(n\xi)=\frac{1}{2\pi i}\oint e^{-n\psi(t)}f(t)\,dt, \tag{4.1}$$

where

$$\psi(t)=\log t-\xi\log\left(\frac{1+t}{1-t}\right),\qquad f(t)=\frac{1}{t}. \tag{4.2}$$

The expansion of $G_n(n\xi)$ for $n\to\infty$ and finite complex ξ will be obtained by application of the method of steepest descents applied to the integral (4.1). Note that although $t=0$ is a branch point of the phase function $\psi(t)$, it is only a pole of the integrand.

In order to deform the contour in (4.1) it is necessary to introduce cuts in the t-plane to make the integrand single-valued. We do this by placing two cuts extending from $t=\pm 1$ to infinity along the positive and negative real axes, although other choices may be more convenient when deforming the integration path. The saddle points t_s of the integrand are given by $\psi'(t)=0$; that is, by $t_s^2+2\xi t_s-1=0$, whereupon

$$t_{s1}=\frac{1}{\xi+\sqrt{1+\xi^2}},\qquad t_{s2}=\frac{1}{\xi-\sqrt{1+\xi^2}}. \tag{4.3}$$

At a saddle t_{sj} we have

$$\psi(t_{sj})=-\log\left(\xi\pm\sqrt{1+\xi^2}\right)-\xi\log\left(\xi^{-1}\pm\sqrt{1+\xi^{-2}}\right), \tag{4.4}$$

where the upper or lower signs correspond to $j=1$ or 2, respectively. Some routine algebra shows that, for ξ in the first quadrant, we have $\arg t_{s1}\in[-\frac{1}{2}\pi,0]$ and $\arg t_{s2}\in[-\pi,-\frac{1}{2}\pi]$. Then, from the elementary properties of the above quadratic in t_s, we find $t_{s1}t_{s2}=e^{-\pi i}$ and $t_{s1}+t_{s2}=2\xi e^{-\pi i}$, whence

$$\psi(t_{s1})+\psi(t_{s2})=\log\left(t_{s1}t_{s2}\right)-\xi\log\left(\frac{1+t_{s1}t_{s2}+t_{s1}+t_{s2}}{1+t_{s1}t_{s2}-t_{s1}-t_{s2}}\right)=\pi i(\xi-1). \tag{4.5}$$

4.1. Topology of the steepest descent paths

Paths of steepest descent from a saddle t_s can terminate only at $t=-1$ or pass to infinity in the directions

$$\arg t=\operatorname{Im}\psi(t_s)\pm\pi\operatorname{Re}(\xi).$$

The topology of the paths of steepest descent when $\xi>0$ is illustrated in Fig. 1. In this case the saddles lie on the real axis, with $0<t_{s1}<1$ and $t_{s2}<-1$. Since $\operatorname{Im}\psi(t_s)=0$, the steepest descent path through the saddle t_{s1} passes to infinity in the directions $\arg t=\pm\pi\xi$ when $\xi<1$. The integration path in (4.1) can then be expanded to coincide with the steepest descent path through t_{s1}, together with the loop described in the negative sense surrounding the branch cut $(-\infty,-1]$ and part of the

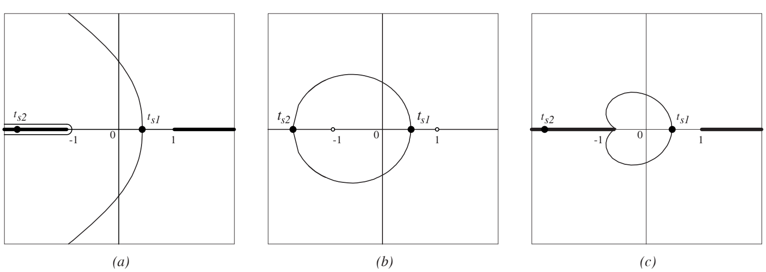

Figure 1: *The steepest descent paths through the saddle t_{s1} for positive values of ξ: (a) $\xi<1$, (b) $\xi=1$ and (c) $\xi>1$. The heavy dots denote the saddle points and the heavy lines are the branch cuts.*

circular arc[3] at infinity. When $\xi=1$, the steepest descent path through t_{s1} connects with the saddle t_{s2} on the negative real axis. The loop from t_{s2} round the branch point $t=-1$ in this case yields no contribution to $G_n(n\xi)$, since $x=n$ and both sides of the loop, taken in opposite directions, cancel. When $\xi>1$, the steepest descent path through t_{s1} encircles the origin and terminates at $t=-1$.

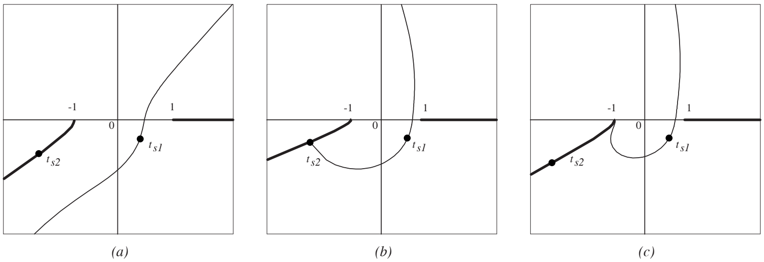

Figure 2: *The steepest descent paths through the saddles t_{s1} and t_{s2} for complex values of ξ: (a) $\xi\in D_1$, (b) $\xi=\xi_I$ and (c) $\xi\in D_2$. The heavy dots denote the saddle points and the heavy lines are the branch cuts. The cut from $t=-1$ coincides with the steepest descent path through t_{s2}.*

When $0<\arg\xi<\frac{1}{2}\pi$, the saddles move into the lower half of the complex plane as shown in Fig. 2. There are three different configurations of the steepest descent paths according as ξ lies in the domains D_1, D_2 of the first quadrant, or on the curve $\xi=\xi_I$ separating these two domains; see Fig. 3. This curve corresponds to points where $\mathrm{Im}\,\psi(t_{s1})=\mathrm{Im}\,\psi(t_{s2})$, so that the steepest descent path through t_{s1} connects with the saddle t_{s2}, as shown in Fig. 2(b). Also shown in Fig. 3 is the (dashed) curve $\xi=\xi_R$ on which $\mathrm{Re}\,\psi(t_{s1})=\mathrm{Re}\,\psi(t_{s2})$ — this includes the part of the imaginary axis satisfying $0<\mathrm{Im}\,\xi\leqslant 1$. As one crosses this latter curve from the lower to the upper side, there is an exchange of dominance between the saddles; for values of ξ below this curve — and *a fortiori* for $\xi\in D_1$ — the saddle t_{s1} is the dominant saddle. Numerical values of ξ_I and ξ_R are displayed in Table 2.

$\mathrm{Re}(\xi_I)$	$\mathrm{Im}(\xi_I)$	$\mathrm{Re}(\xi_I)$	$\mathrm{Im}(\xi_I)$	$\mathrm{Re}(\xi_R)$	$\mathrm{Im}(\xi_R)$	$\mathrm{Re}(\xi_R)$	$\mathrm{Im}(\xi_R)$
0	1.00000	0.60	0.54092	0	1.00000	1.40	1.54510
0.05	0.97056	0.70	0.43159	0.20	1.10736	1.60	1.59776
0.10	0.93993	0.75	0.37155	0.40	1.20111	1.80	1.64678
0.20	0.87469	0.80	0.30741	0.60	1.28422	2.00	1.69260
0.30	0.80339	0.90	0.16503	0.80	1.35881	2.20	1.73561
0.40	0.72495	0.95	0.08568	1.00	1.42642	2.50	1.79551
0.50	0.63801	1.00	0.00000	1.20	1.48822	3.00	1.88510

Table 2: *Values of ξ_I and ξ_R.*

[3] The circular arc at infinity makes no contribution since the integrand in (4.1) behaves like t^{-n-1} for large $|t|$.

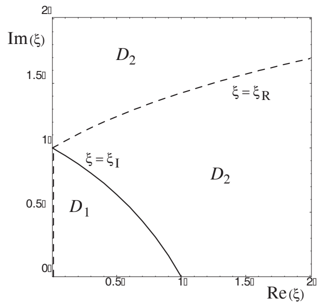

Figure 3: *The domains D_1 and D_2 in the ξ-plane and the boundary curve $\xi = \xi_I$ corresponding to a Stokes phenomenon. The dashed curve (including part of the imaginary ξ-axis satisfying $0 < Im(\xi) \leqslant 1$) indicates the values of $\xi = \xi_R$ corresponding to an exchange of dominance between the saddles; for values of ξ below this curve the dominant saddle is t_{s1}.*

Then, for $\xi \in D_1$, the steepest descent path through t_{s1} passes to infinity in both directions, whereas that through t_{s2} has one half that terminates at $t = -1$ with the other half passing to infinity;[4] see Fig. 2(a). In this case, it is more convenient to place the branch cut emanating from $t = -1$ to coincide with the steepest descent path through t_{s2}. The closed path around the origin can then be formed by taking the steepest descent path through t_{s1}, together with a loop described in the negative sense surrounding this latter branch cut and parts of the circular arc at infinity. When $\xi \in D_2$, one half of the steepest descent path through t_{s1} terminates at $t = -1$ with the other half passing to infinity. The closed circuit is then formed by taking this latter path together with part of a large circular arc at infinity and the upper side of the branch cut emanating from $t = -1$.

Finally, when $\arg \xi = \frac{1}{2}\pi$, the saddles are distributed symmetrically about the negative imaginary t-axis for $|\xi| < 1$, coalesce to form a double saddle at $t = -i$ when $\xi = i$ and are both situated on the negative imaginary t-axis when $|\xi| > 1$; see Fig. 4, where the branch cuts have been placed on the real axis. We note that the steepest descent path through t_{s2} cannot terminate at $t = -1$ in this case, since as $t \to -1$

$$\operatorname{Im} \psi(t) \sim -|\xi| \log(1+t) \to +\infty,$$

and so must loop round the point $t = -1$ and pass to infinity on the adjacent Riemann sheet.

To determine the steepest descent paths through t_{s1} and t_{s2}, we set $\xi = i|\xi|$ and write $t = re^{i\phi}$ to find

$$\operatorname{Im} \psi(t) = \phi - |\xi| \log\left(\frac{1+r^2+2r\cos\phi}{1+r^2-2r\cos\phi}\right).$$

[4]When Im $(\xi) \neq 0$, the steepest descent path through t_{s2} approaches the point $t = -1$ in a spiral. In certain cases it is possible for the path through t_{s1} to bend round the branch point $t = 1$ and pass to infinity on an adjacent Riemann sheet of $\psi(t)$.

Then, with $\mathrm{Im}\,\psi(t_{s1})=\phi_1$, the steepest descent path through t_{s1} is described by

$$r=\varepsilon\cos\phi\pm\sqrt{\varepsilon^2\cos^2\phi-1},\qquad \varepsilon\equiv\varepsilon(\phi)=\frac{\chi+1}{\chi-1},\quad \chi=\exp\left(\frac{2(\phi-\phi_1)}{|\xi|}\right).$$

These paths are illustrated in Fig. 4 in particular cases; the mirror image of the curves give the steepest descent paths through t_{s2}. The circuit is then closed by adding portions of the circular arc at infinity.

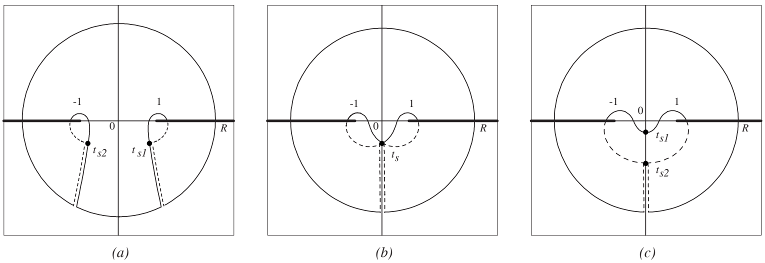

Figure 4: *The steepest descent paths through the saddles for purely imaginary values of* ξ*: (a)* $|\xi|<1$*, (b)* $|\xi|=1$ *and (c)* $|\xi|>1$*. The heavy dots denote the saddle points and the heavy lines are the branch cuts. The dashed portions of the descent paths lie on adjacent Riemann sheets.*

It should be noted that the dashed parts of these paths lie on adjacent Riemann sheets of $\psi(t)$. Thus, for example, in Fig. 4(a) when the path has crossed over the branch cut emanating from $t=1$, we have $\log(1-t)$ replaced by $\log(1-t)-2\pi i$. This results in the value of $e^{-n\psi(t)}$ at t_{s1} on the adjacent sheet being a factor $e^{-2\pi n\mathrm{Im}(\xi)}$ smaller than that at t_{s1} on the principal sheet. A similar consideration applies to the steepest descent path through t_{s2}. In Fig. 4(b), both halves of the steepest descent path through t_{s1} approach t_{s2} on different adjacent sheets of $\psi(t)$, with the result that the value of $e^{-n\psi(t)}$ at t_{s2} is a factor $e^{-2\pi n\mathrm{Im}(\xi)}$ smaller than that at t_{s2} on the principal sheet. We remark that the steepest descent paths in Fig. 4 are essentially the same (but rotated through $-\pi/2$ and with branch cuts placed differently) as those depicted in Figs. 15, 16 in [6] in the discussion of the Meixner–Pollaczek polynomials.

From these considerations, it is seen that both saddles contribute when $\xi\in D_1$, whereas only the saddle t_{s1} contributes when $\xi\in D_2$. On the boundary separating these two domains, $\xi=\xi_I$, we encounter a Stokes phenomenon, where the subdominant contribution I_2 switches off as ξ crosses from D_1 to D_2. On $\arg\xi=\frac{1}{2}\pi$ with $|\xi|<1$, the expansions I_1 and I_2 (defined below) are of equal magnitude.

4.2. The expansion for $n\to\infty$

From (4.2) and (4.3), we have

$$\psi''(t_{sj})=-\frac{(\xi+t_{sj})}{\xi t_{sj}^2}=\mp\frac{\sqrt{1+\xi^2}}{\xi t_{sj}^2},$$

where the upper or lower sign corresponds to $j=1$ or 2, respectively. The direction of the steepest descent path at the saddle t_{sj} is $-\frac{1}{2}\arg\psi''(t_{sj})$, where $|\arg\psi''(t_{sj})|<\pi$.

The contributions $I_1(\xi)$ and $I_2(\xi)$ from the steepest descent paths through the saddle points t_{s1} and t_{s2}, respectively, are then given by

$$I_j(\xi) \sim \frac{e^{-n\psi(t_{sj})}}{it_{sj}\sqrt{2\pi\,\psi''(t_{sj})}} \sum_{m=0}^{\infty} \frac{c_m^{(j)}\Gamma(m+\frac{1}{2})}{n^{m+\frac{1}{2}}\Gamma(\frac{1}{2})}$$

$$= \frac{e^{-n\psi(t_{sj})}}{\sqrt{2\pi}} \frac{i^{1-j}\xi^{\frac{1}{2}}}{(1+\xi^2)^{\frac{1}{4}}} \sum_{m=0}^{\infty} \frac{c_m^{(j)}\Gamma(m+\frac{1}{2})}{n^{m+\frac{1}{2}}\Gamma(\frac{1}{2})} \qquad (j=1,2) \tag{4.6}$$

as $n\to\infty$, where the coefficients $c_0^{(j)}=1$ and [8, p. 127], [4, p. 119]

$$c_1^{(j)} = \frac{1}{\psi''}\left\{\frac{f''}{f} - \frac{\psi''' f'}{\psi'' f} + \frac{1}{4}\left(\frac{5\psi'''^2}{3\psi''^2} - \frac{\psi^{iv}}{\psi''}\right)\right\},$$

$$c_2^{(j)} = \frac{1}{\psi''^2}\left\{\frac{f^{iv}}{6f} - \frac{5\psi''' f'''}{9\psi'' f} + \frac{5}{12}\left(\frac{7\psi'''^2}{3\psi''^2} - \frac{\psi^{iv}}{\psi''}\right)\frac{f''}{f} - \frac{35}{36}\left(\frac{\psi'''^3}{\psi''^3} - \frac{\psi'''\psi^{iv}}{\psi''^2} + \frac{6\psi^{v}}{35\psi''}\right)\frac{f'}{f}\right.$$
$$\left. + \frac{35}{36}\left(\frac{11\psi'''^4}{24\psi''^4} - \frac{3}{4}\left(\frac{\psi'''^2}{\psi''^2} - \frac{\psi^{iv}}{6\psi''}\right)\frac{\psi^{iv}}{\psi''} + \frac{\psi'''\psi^{v}}{5\psi''^2} - \frac{\psi^{vi}}{35\psi''}\right)\right\},$$

with ψ, f and their derivatives being evaluated at $t=t_{sj}$; see also [10, p. 13]. This yields the values

$$c_1^{(1)} = -c_1^{(2)} = -\frac{(2-\xi^2+2\xi^4)}{12\xi(1+\xi^2)^{3/2}}, \qquad c_2^{(1)} = c_2^{(2)} = \frac{4+365\xi^4(1+\xi^2)+4\xi^{10}}{864\xi^2(1+\xi^2)^4}.$$

Then, upon use of (4.5), we obtain the expansions valid for ξ bounded away from zero

$$I_1(\xi) \sim \frac{\lambda^n}{\sqrt{2\pi}} \frac{\xi^{\frac{1}{2}}}{(1+\xi^2)^{\frac{1}{4}}} \sum_{m=0}^{\infty} \frac{c_m^{(1)}\Gamma(m+\frac{1}{2})}{n^{m+\frac{1}{2}}\Gamma(\frac{1}{2})} \tag{4.7}$$

and

$$I_2(\xi) \sim (-)^n \frac{\lambda^{-n}e^{-\pi i n\xi}}{i\sqrt{2\pi}} \frac{\xi^{\frac{1}{2}}}{(1+\xi^2)^{\frac{1}{4}}} \sum_{m=0}^{\infty} \frac{c_m^{(2)}\Gamma(m+\frac{1}{2})}{n^{m+\frac{1}{2}}\Gamma(\frac{1}{2})}, \tag{4.8}$$

where, by (4.4),

$$\lambda \equiv e^{-\psi(t_{s1})} = (\xi+\sqrt{1+\xi^2})(\xi^{-1}+\sqrt{1+\xi^{-2}})^{\xi}.$$

The expansions $I_1(\xi)$ and $I_2(\xi)$ in (4.7) and (4.8) cease to be valid in the neighbourhood of the point $\xi=i$, where the saddles coalesce.

When $0<\xi<1$, we may collapse the loop onto the negative real axis to find the expansion

$$G_n(n\xi) \sim I_1(\xi) + \frac{\sin(\pi n\xi)}{\pi}(-)^{n-1}I_2(\xi) \qquad (\xi\in(0,1)) \tag{4.9}$$

as $n\to\infty$. When $\xi\in D_1$ (with $\arg\xi\neq 0$), the contribution from the upper side of the branch cut emanating from $t=-1$ and coincident with the steepest descent path through t_{s2} is a factor $e^{-2\pi n\mathrm{Im}(\xi)}$ smaller than $I_2(\xi)$ resulting from the lower side on the principal sheet, and so may be neglected. When $\xi\in D_2$, the contribution $e^{-2\pi n\mathrm{Im}(\xi)}I_2(\xi)$ is also exponentially smaller than $I_1(\xi)$. This conclusion follows from the fact that

$$2\pi\mathrm{Im}(\xi)+\mathrm{Re}\,\psi(t_{s2})=\pi\mathrm{Im}(\xi)-\mathrm{Re}\,\psi(t_{s1})>\mathrm{Re}\,\psi(t_{s1})$$

by (4.5), since as shown in the Appendix, $\mathrm{Re}\,\psi(t_{s1})<0$ for $0\leqslant\arg\xi\leqslant\frac{1}{2}\pi$. Then we have the expansion of $G_n(n\xi)$ given by

$$G_n(n\xi)\sim\begin{cases}I_1(\xi)+I_2(\xi) & (\xi\in D_1')\\ I_1(\xi) & (\xi\in D_2')\end{cases}\tag{4.10}$$

as $n\to\infty$, where the prime on D_1 and D_2 denotes the deletion of the neighbourhood of the point $\xi=i$ and, in the case of D_1, also the interval $0<\xi<1$.

4.3. Particular cases

When $\arg\xi=\frac{1}{2}\pi$, we replace ξ by $i\xi$ $(\xi>0)$ to find after some routine algebra

$$\psi(t_{s1})+\tfrac{1}{2}\pi\xi+\tfrac{1}{2}\pi i=\begin{cases}i\theta-i\xi\log(\xi^{-1}+\sqrt{\xi^{-2}-1}) & (0<\xi<1)\\ -\theta+\xi\arctan\sqrt{\xi^2-1} & (\xi>1),\end{cases}$$

where θ is defined in (2.2). Then from (4.7), (4.8) and (4.10) we obtain the non-uniform expansions valid for $n\to\infty$

$$G_n(in\xi)\sim\begin{cases}\dfrac{2i^n}{\sqrt{2\pi n}}\dfrac{\xi^{\frac{1}{2}}e^{\frac{1}{2}\pi n\xi}}{(1-\xi^2)^{\frac{1}{4}}}\left\{\sin\Psi_n\displaystyle\sum_{m=0}^\infty\frac{c_{2m}^{(1)}}{n^{2m}}\frac{\Gamma(2m+\frac{1}{2})}{\Gamma(\frac{1}{2})}\right.\\ \qquad\qquad\left.+i\cos\Psi_n\sum_{m=0}^\infty\frac{c_{2m+1}^{(1)}}{n^{2m+1}}\frac{\Gamma(2m+\frac{3}{2})}{\Gamma(\frac{1}{2})}\right\}\\ \qquad\qquad(0<\xi<1)\\ \dfrac{i^n}{\sqrt{2\pi n}}\dfrac{\xi^{\frac{1}{2}}e^{\frac{1}{2}\pi n\xi}}{(\xi^2-1)^{\frac{1}{4}}}\exp[n(\theta-\xi\arctan\sqrt{\xi^2-1})]\displaystyle\sum_{m=0}^\infty\frac{c_m^{(1)}}{n^m}\frac{\Gamma(m+\frac{1}{2})}{\Gamma(\frac{1}{2})}\\ \qquad\qquad(\xi>1),\end{cases}\tag{4.11}$$

where

$$\Psi_n\equiv n\theta-n\xi\log(\xi^{-1}+\sqrt{\xi^{-2}-1})+\tfrac{1}{4}\pi$$

and we have made the conjecture that the coefficients satisfy $c_m^{(1)}=(-)^m c_m^{(2)}$ $(m\geqslant 1)$. The leading terms of these expansions agree with the corresponding expressions in (2.1).

In the particular case $\xi = 1$, the dominant behaviour of $G_n(n)$ is given by $I_1(1)$. Upon evaluation of the coefficients $c_1^{(1)}$ and $c_2^{(1)}$, we find the expansion

$$G_n(n) \sim \frac{2^{-\frac{1}{4}}}{\sqrt{2\pi n}}(1+\sqrt{2})^{2n}\left(1 - \frac{2^{\frac{1}{2}}}{32n} + \frac{123}{3072n^2} + \cdots\right) \qquad (n \to \infty). \tag{4.12}$$

This case can be verified by observing that from (3.5)

$$G_n(n) = 2^{-n}{}_2F_1\left(\left.\begin{matrix} n+1, n \\ 1 \end{matrix}\right| \tfrac{1}{2}\right) = {}_2F_1\left(\left.\begin{matrix} -n, n \\ 1 \end{matrix}\right| -1\right)$$

by means of the well-known transformation in [9, Eq. (15.8.1)]. The first three terms in the expansion of ${}_2F_1(-n, n; 1; -1)$ as $n \to \infty$ can be obtained from [14, p. 289] and are found to agree[5] with (4.12).

The results of numerical calculations of $G_n(n\xi)$ for different n and ξ are presented in Table 3, which shows the absolute value of the relative error using the truncation index $m = 2$ in the expansions $I_1(\xi)$ and $I_2(\xi)$. The expansion $I_2(\xi)$ is subdominant in D_1, becoming comparable with $I_1(\xi)$ only in the neighbourhood of the imaginary ξ-axis.

ξ	$n=50$	$n=80$	ξ	$n=50$	$n=80$
0.50	2.254×10^{-7}	5.531×10^{-8}	$0.5+0.5i$	1.327×10^{-6}	3.180×10^{-7}
0.75	2.466×10^{-7}	6.000×10^{-8}	$0.5+1.0i$	9.377×10^{-6}	2.247×10^{-6}
1.00	1.975×10^{-7}	4.800×10^{-8}	$1.0+0.5i$	2.926×10^{-7}	7.091×10^{-8}
1.25	1.241×10^{-7}	3.021×10^{-8}	$1.0+1.0i$	4.544×10^{-7}	1.102×10^{-8}
1.50	7.195×10^{-8}	1.754×10^{-8}	$0.5i$	1.342×10^{-6}	2.385×10^{-6}
2.00	2.836×10^{-8}	6.941×10^{-9}	$1.5i$	1.019×10^{-5}	2.567×10^{-6}

Table 3: *The absolute value of the relative error in the computation of $G_n(n\xi)$ by means of (4.9) and (4.10) with truncation index $m=2$.*

Acknowledgement

The author acknowledges some helpful comments made by the referees.

Appendix: The proof that $\mathrm{Re}\,\psi(t_{s1}) < 0$ for $0 \leqslant \arg\xi \leqslant \frac{1}{2}\pi$

We establish that $\mathrm{Re}\,\psi(t_{s1}) < 0$ when $0 \leqslant \arg\xi \leqslant \frac{1}{2}\pi$ ($\xi \neq 0$). From (4.4), we have

$$\begin{aligned} -\psi(t_{s1}) &= \log(\xi + \sqrt{1+\xi^2}) + \xi \log(\xi^{-1} + \sqrt{1+\xi^{-2}}) \\ &= \operatorname{arcsinh}(\xi) + \xi \operatorname{arcsinh}(\xi^{-1}). \end{aligned}$$

[5] The quantity N appearing in the expression for the coefficient c_1 in [14, p. 285] is incorrect: this should read $N = (\alpha+\beta-1)^2 + \alpha - \beta - \frac{1}{2}$.

Let $Z = \text{arcsinh}\,(z)$, $Z = \alpha + i\beta$ with $|\arg z| \leqslant \frac{1}{2}\pi$. The mapping $z \mapsto Z$ is shown in Fig. 5. We have $\alpha = 0$ when z is situated on the imaginary axis between $[-i, i]$, with $\alpha > 0$ elsewhere. The imaginary part of Z satisfies $\beta > 0$ (resp. < 0) according as z is in the upper (resp. lower) half-plane, with $\beta = 0$ when $\arg z = 0$.

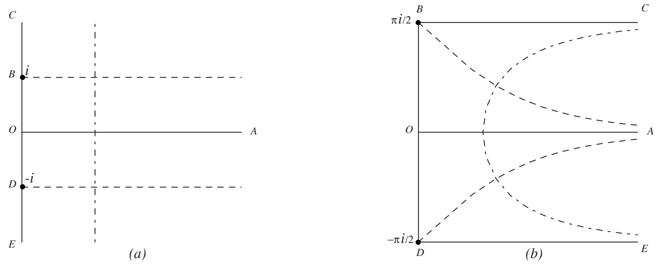

Figure 5: *The mapping $Z = \text{arcsinh}\,(z)$ for $|\arg z| \leqslant \frac{1}{2}\pi$: (a) the z-plane and (b) the Z-plane.*

We now put $\text{arcsinh}\,(\xi) = u + iv$ and $\text{arcsinh}\,(\xi^{-1}) = u' - iv'$,where u, u', v and v' are real. Then, when $0 \leqslant \arg \xi < \frac{1}{2}\pi$ $(\xi \neq 0)$, $u > 0$, $u' > 0$, $v > 0$ and $v' > 0$. When $\arg \xi = \frac{1}{2}\pi$, we have $u = 0$ for $0 < \text{Im}\,(\xi) \leqslant 1$ and $u' = 0$ for $\text{Im}\,(\xi) > 1$, the other quantities being positive in both cases. Hence

$$-\text{Re}\,\psi(t_{s1}) = u + \text{Re}\,[\xi\,(u' - iv')]$$
$$= u + u'\,\text{Re}\,(\xi) + v'\,\text{Im}\,(\xi).$$

Thus, $\text{Re}\,\psi(t_{s1})$ is seen to be negative for $0 \leqslant \arg \xi \leqslant \frac{1}{2}\pi$ $(\xi \neq 0)$. It therefore follows that the contribution $I_1(\xi)$ from the saddle t_{s1} is exponentially large as $n \to \infty$ for $0 \leqslant \arg \xi \leqslant \frac{1}{2}\pi$ $(\xi \neq 0)$.

REFERENCES

[1] H. BATEMAN, *The polynomial of Mittag-Leffler*, Proc. N. A. S. **26** (1940), 491–496.

[2] H. BATEMAN, *An orthogonal property of the hypergeometric polynomial*, Proc. N. A. S. **28** (1942), 374–377.

[3] N. BLEISTEIN AND R. A. HANDELSMAN, *Asymptotic Expansion of Integrals*, Dover, New York, 1986.

[4] R. B. DINGLE, *Asymptotic Expansions: Their Derivation and Interpretation*, Academic Press, London, 1973.

[5] T. X. HE, L. C. HSU AND P. J.-S. SHIUE, *The Scheffer group and the Riordan group*, Discrete Appl. Math. **155** (2007), 1895–1909.

[6] X. LI AND R. WONG, *On the asymptotics of the Meixner-Pollaczek polynomials and their zeros*, Constr. Approx. **17** (2001), 59–90.

[7] Y. L. LUKE, *The Special Functions and Their Approximations*, Vol. 1, Academic Press, New York, 1969.

[8] F. W. J. OLVER, *Asymptotics and Special Functions*, Academic Press, New York, 1974. Reprinted in A. K. Peters, Massachussets, 1997.

[9] F. W. J. OLVER, D. W. LOZIER, R. F. BOISVERT AND C. W. CLARK (EDS.), *NIST Handbook of Mathematical Functions*, Cambridge University Press, Cambridge, 2010.

[10] R. B. PARIS, *Hadamard Expansions and Hyperasymptotic Evaluation: an Extension of the Method of Steepest Descents*, Encyclopedia of Mathematics, vol. 141, Cambridge University Press, Cambridge, 2011.

[11] S. ROMAN, *The Umbral Calculus*, Academic Press, New York, 1984.
[12] G. RZĄDKOWSKI, *On some expansions, involving falling factorials, for the Euler gamma function and the Riemann zeta function*, arXiv.org/abs/1007.1955v1 (2010).
[13] M. S. STANKOVIĆ, S. D. MARINKOVIĆ AND P. M. RAJKOVIĆ, *Deformed Mittag-Leffler polynomials*, arXiv.org/abs/1007.3612v1 (2010).
[14] G. N. WATSON, *Asymptotic expansions of hypergeometric functions*, Trans. Cambridge Phil. Soc. **22** (1918), 277–308.
[15] E. T. WHITTAKER AND G. N. WATSON, *Modern Analysis*, Cambridge University Press, Cambridge 1952.
[16] R. WONG, *Asymptotic Expansion of Integrals*, Academic Press, London, 1989.

(Received May 28, 2011)

R. B. Paris
University of Abertay Dundee
Dundee DD1 1HG
UK